

Beyond-mean-field analysis of the Townes soliton and its breathing mode

D. S. Petrov¹

Université Paris-Saclay, CNRS, LPTMS, 91405 Orsay, France

* dmitry.petrov@universite-paris-saclay.fr

December 22, 2024

Abstract

By using the Bogoliubov perturbation theory we describe the self-bound ground state and excited breathing states of N two-dimensional bosons with zero-range attractive interactions. Our results for the ground state energy B_N and size R_N improve previously known large- N asymptotes and we better understand the crossover to the few-body regime. The oscillatory breathing motion results from the quantum-mechanical breaking of the mean-field scaling symmetry. The breathing-mode frequency scales as $\Omega \propto |B_N|/\sqrt{N}$ at large N .

Contents

1	Introduction	1
2	Mean-field description	2
3	Beyond-mean-field analysis	3
3.1	Ground-state properties	5
3.2	Breathing dynamics	6
4	Discussion	7
5	Summary	9
A	Determination of c_1	10
	References	11

1 Introduction

At the mean-field level the problem of two-dimensional attractive bosons is governed by the nonlinear Schrödinger equation with cubic nonlinearity. Its localized stationary solution, called Townes soliton, was found by Chiao and co-workers who studied propagation of optical beams in dielectric materials [1]. Townes solitons have a few peculiar properties related to the scale invariance of the underlying classical mean-field theory [2] (see also [3]).

Namely, the soliton is stationary only when the coupling constant g takes a critical value g_c related to the norm of the wave function N by $g_c N = -\pi C$, where $C = 1.862$. For $g < g_c$ the soliton collapses and for $g > g_c$ it expands. These features have recently been observed in ultra-cold gas experiments [4–6]. Exactly at $g = g_c$ one can generate an infinite number of stationary states by rescaling a unique dimensionless Townes profile by an arbitrary scaling factor. For all these stationary solutions the mean-field energy vanishes [7, 8]. In other words, the mean-field theory leaves the size of the soliton undefined and predicts zero for its energy and for its breathing (or monopole) mode frequency.

A different scenario is suggested by various exact results obtained for finite N [9–17]. It is established that the trimer and the tetramer have two (ground and excited) self-bound states with finite energies $B_3^{(0)} = 16.522688(1)B_2$, $B_3^{(1)} = 1.2704091(1)B_2$ [13] and $B_4^{(0)} = 197.3(1)B_2$, $B_4^{(1)} = 25.5(1)B_2$ [14], respectively. Here, $B_2 < 0$ is the energy of the dimer and we denote ground and excited states, respectively, by superscripts (0) and (1).

Hammer and Son [13] predicted that the energy and the size of the ground state should scale respectively as $B_N \sim B_2 e^{4N/C}$ and $R_N \sim R_2 e^{-2N/C}$ for large N . Their theory is based on the idea that the *renormalized* coupling constant g runs logarithmically with the system size and, therefore, breaks the mean-field scale invariance. Bazak and Petrov [17] have calculated ground-state energies for up to $N = 26$ particles confirming the exponential scaling of Ref. [13]. Moreover, they attempted to fit the results with the ansatz $B_N = B_2 e^{2N/C + c_1 + c_2/N + \dots}$ arriving at $c_1 \approx -2.06$.

Little is known about excited states for $N > 4$. It is however quite natural to assume (particularly looking at the problem within the hyperspherical formalism [16]) that the $(0) \rightarrow (1)$ excitation is a precursor of the breathing mode. The finite value of $B_N^{(1)} - B_N^{(0)}$ is thus a beyond-mean-field effect and it emerges as a clear experimentally testable indicator of a quantum anomaly which breaks the mean-field scale symmetry. Olshanii and co-workers [18] proposed to observe this anomaly in a trapped repulsive Bose gas, arguing that the breathing-mode frequency should deviate from two times the trap frequency.

In this paper we develop the Bogoliubov perturbation theory for the two-dimensional soliton. The theory confirms that in the limit of large N the quantity $\ln(B_N/B_2) - 2N/C$ indeed tends to a constant c_1 [19]. Our numerical diagonalization of the Bogoliubov-de Gennes equations and calculation of the leading beyond-mean-field correction gives $c_1 = -1.91(1)$. We then discuss the breathing mode of the soliton. Introducing the soliton radius as a collective variable we derive the corresponding equation of motion and obtain for the breathing-mode frequency $\hbar\Omega = 3.804|B_N|/\sqrt{N}$. Our results give quantitative basis for observing quantum effects in droplets with large but finite N .

2 Mean-field description

The mean-field description of N two-dimensional bosons with contact attraction is obtained from the Lagrangian density

$$\mathcal{L}(\Psi, \Psi^*) = \text{Re}[i\Psi^*(\boldsymbol{\rho}, t)\partial_t\Psi(\boldsymbol{\rho}, t)] - |\nabla_{\boldsymbol{\rho}}\Psi(\boldsymbol{\rho}, t)|^2/2 - g|\Psi(\boldsymbol{\rho}, t)|^4/2, \quad (1)$$

where the coupling constant g is negative, the field Ψ is normalized as $\int d^2\rho |\Psi(\boldsymbol{\rho}, t)|^2 = N$, and we set $\hbar = m = 1$. The equation of motion corresponding to Eq. (1) is the Gross-Pitaevskii equation

$$i\partial_t\Psi(\boldsymbol{\rho}, t) = -(1/2)\nabla_{\boldsymbol{\rho}}^2\Psi(\boldsymbol{\rho}, t) + g|\Psi(\boldsymbol{\rho}, t)|^2\Psi(\boldsymbol{\rho}, t), \quad (2)$$

which, for $g = g_c = -\pi C/N$ allows for a family of nodeless stationary solutions

$$\Psi_R(\boldsymbol{\rho}, t) = e^{it/(2R^2)}\Psi_R(\boldsymbol{\rho}) = e^{it/(2R^2)}\sqrt{N/(2\pi C)}f(\boldsymbol{\rho}/R)/R. \quad (3)$$

The dimensionless Townes profile f is a unique nodeless real solution of [1]

$$f''(r) + f'(r)/r + f(r)^3 = f(r). \quad (4)$$

It has a bell-like shape with radius of order one and it satisfies the relations

$$C := \int_0^\infty dr r f^2(r) = \int_0^\infty dr r [f'(r)]^2 = \frac{1}{2} \int_0^\infty dr r f^4(r) = 1.862 \quad (5)$$

and

$$M_2 := \int_0^\infty dr r^3 f^2(r) = 2.211. \quad (6)$$

Using Eqs. (3) and (5) one can show that the mean-field energy functional

$$E_{\text{MF}} = (1/2) \int d^2\rho [|\nabla_\rho \Psi(\rho, t)|^2 + g|\Psi(\rho, t)|^4] \quad (7)$$

indeed vanishes independent of the size R when $g = g_c$ and $\Psi = \Psi_R$. In fact, when an arbitrary initial wave function is allowed to evolve according to Eq. (2), the mean square radius of the corresponding density profile evolves according to $\partial_t^2 \sigma^2 = 4E_{\text{MF}}$, where E_{MF} is the (conserved) mean-field energy given by Eq. (7) [2, 3, 7, 8]. This is why for stationary solutions (3) the energy is necessarily zero. We note however that to extract an atom from the droplet requires energy $-\mu = 1/(2R^2)$. The chemical potential μ can be deduced either from the explicit time dependence $e^{-i\mu t}$ in Eq. (3) or by calculating the derivative $\mu = \partial_N E_{\text{MF}}$ at fixed g and R .

Let us discuss the mean-field breathing dynamics of the Townes soliton, which can be initiated, for instance, by changing g [5]. Consider the ansatz

$$\Psi(\rho, t) = \sqrt{N/(2\pi C)} e^{i\theta(\rho, t)} f[\rho/R(t)]/R(t), \quad (8)$$

where θ is real and the trajectory $R(t)$ is for the moment arbitrary. We substitute Eq. (8) into the Lagrangian density (1) and minimize the action $S = \int \mathcal{L} d^2\rho dt$ with respect to the field $\theta(\rho, t)$. This gives the continuity equation

$$\partial_t |\Psi|^2 + \nabla_\rho (|\Psi|^2 \nabla_\rho \theta) = 0, \quad (9)$$

which is solved by

$$\theta(\rho, t) = [\dot{R}(t)/R(t)]\rho^2/2 - \mu't. \quad (10)$$

The action then becomes

$$S_{\text{MF}} = \int dt \left\{ NM_2 \dot{R}^2(t)/(2C) - (g - g_c)N^2/[2\pi C R^2(t)] + \mu'N \right\}. \quad (11)$$

It describes the classical motion of a particle with coordinate R and mass NM_2/C in the potential $(g - g_c)N^2/(2\pi C R^2)$. The general solution of the corresponding equation of motion reads $R(t) = \sqrt{(g - g_c)N/(\pi A) + A(t - t_0)^2/M_2}$, where A and t_0 are fixed by the initial conditions. For instance, setting $\dot{R}(0) = 0$ gives the trajectory $R(t) = \sqrt{R^2(0) + (g - g_c)Nt^2/[\pi R^2(0)M_2]}$, which describes expansion for $g > g_c$ or collapse otherwise. For $g = g_c$ the system admits the solution $R(t) = R(0) + Vt$ with arbitrary velocity V .

3 Beyond-mean-field analysis

We now turn to the quantum case and consider the Hamiltonian

$$\hat{H} = \frac{1}{2} \int d^2\rho (-\hat{\Psi}_\rho^\dagger \nabla_\rho^2 \hat{\Psi}_\rho + g \hat{\Psi}_\rho^\dagger \hat{\Psi}_\rho^\dagger \hat{\Psi}_\rho \hat{\Psi}_\rho), \quad (12)$$

where $\hat{\Psi}_\rho^\dagger$ is the operator creating a boson at position ρ . We would like to calculate the leading correction to the energy of the system perturbatively at $g = g_c$ using the stationary state (3) as the unperturbed solution.

The standard Bogoliubov theory consists of writing $\hat{\Psi}_\rho = \Psi_R(\rho) + \delta\hat{\Psi}_\rho$ and expanding (12) up to second-order terms in powers of $\delta\hat{\Psi}$ and $\delta\hat{\Psi}^\dagger$. The zero-order term is the mean-field energy functional (7) and the first-order terms are absent since we have chosen the condensate wave function satisfying the Gross-Pitaevskii equation. The quadratic Bogoliubov Hamiltonian can be written as

$$\hat{H}_2 = \frac{1}{2} \int d^2\rho \begin{pmatrix} \delta\hat{\Psi}_\rho^\dagger & \delta\hat{\Psi}_\rho \end{pmatrix} \begin{pmatrix} \hat{A} & \hat{B} \\ \hat{B} & \hat{A} \end{pmatrix} \begin{pmatrix} \delta\hat{\Psi}_\rho \\ \delta\hat{\Psi}_\rho^\dagger \end{pmatrix} - \text{Tr}(\hat{A})/2, \quad (13)$$

where $\hat{A} = -\nabla_\rho^2/2 - \mu + 2g_c\Psi_R^2(\rho)$, $\hat{B} = g_c\Psi_R^2(\rho)$, and we use the fact that $\Psi_R(\rho)$ is real. This quadratic Hamiltonian is diagonalized by solving the Bogoliubov-de Gennes equations

$$\begin{pmatrix} \hat{A} & \hat{B} \\ -\hat{B} & -\hat{A} \end{pmatrix} \begin{pmatrix} u_\nu(\rho) \\ v_\nu(\rho) \end{pmatrix} = \epsilon_\nu \begin{pmatrix} u_\nu(\rho) \\ v_\nu(\rho) \end{pmatrix}. \quad (14)$$

General properties of matrices of type Eq. (14) can be found in the textbook of Blaizot and Ripka [20]. In our particular case, the spectrum is real and for each eigenstate ν with $\epsilon_\nu > 0$ there is an eigenstate η with $\epsilon_\eta = -\epsilon_\nu$. The ground state energy of \hat{H}_2 equals

$$E_{\text{BMF}} = \sum_{\nu: \epsilon_\nu > 0} \epsilon_\nu/2 - \text{Tr}(\hat{A})/2. \quad (15)$$

A peculiarity of the Bogoliubov spectrum in our case is that Eq. (14) has four pairs of eigenstates with $\epsilon = 0$. They correspond to four zero modes related to arbitrary changes of the complex phase of the condensate wave function [$U(1)$ symmetry], arbitrary shifts of the system in two spatial directions (translational symmetry), and arbitrary changes of R (Pitaevskii-Rosch scale symmetry). These modes describe motion without restoring force resembling the harmonic oscillator $\hat{p}^2/2 + \omega^2\hat{x}^2/2$ with vanishing frequency ω . The main conceptual problem here is that the classical symmetry-broken state (say, localized at $x = 0$ and $p = 0$) is very different from the quantum-mechanical ground $p = 0$ state, completely delocalized in space. The problem has been discussed in detail in Ref. [20] (see also [21, 22]). Starting with the classical $x = p = 0$ ground state and evolving it with the Hamiltonian $\hat{p}^2/2$ one observes diffusion of x . Note, however, that although the linearized theory is formally restricted to small fluctuations around the classical ground state, it does predict the correct (vanishing) energy of the true delocalized state. In other words, we can still use Eq. (15) to predict the energy of the soliton. As long as we are not interested in diffusion effects, the fact that $\Psi_R(\rho)$ breaks the symmetries does not prevent from determining the energy. We will return to this point in Sec. 4.

Equation (15) represents a diverging sum. The divergence comes from large momenta and, therefore, can be understood from the local-density analysis when we assume that the system is locally homogeneous. Substituting the local Bogoliubov spectrum $\epsilon_p =$

$\sqrt{[p^2/2 - \mu + 2g_c\Psi_R^2(\boldsymbol{\rho})]^2 - g_c^2\Psi_R^4(\boldsymbol{\rho})}$ into Eq. (15) and averaging over space gives

$$\begin{aligned} E_{\text{BMF,LDA}} &= \frac{1}{2} \int d^2\rho \int \frac{d^2p}{(2\pi)^2} \{ \epsilon_p - [p^2/2 - \mu + 2g_c\Psi_R^2(\boldsymbol{\rho})] \} \\ &= -\frac{1}{2} \int d^2\rho \int \frac{d^2p}{(2\pi)^2} \left[\frac{g_c^2\Psi_R^4(\boldsymbol{\rho})}{p^2} + O(p^{-4}) \right], \end{aligned} \quad (16)$$

where the second line explicitly shows the logarithmic divergence. This divergence can be regularized by introducing a momentum cutoff for the interaction. Here we choose an equivalent approach more convenient for numerical analysis. Namely, we put the system on a square lattice with spacing h such that $\boldsymbol{\rho}$ runs over the nodes denoted by integers i and j . The Laplacian $\nabla_{\boldsymbol{\rho}}^2$ in Eq. (12) and in the operator \hat{A} is replaced by the lattice Laplacian defined by

$$\hat{L}_h \Phi_{i,j} = (\Phi_{i+1,j} + \Phi_{i-1,j} + \Phi_{i,j+1} + \Phi_{i,j-1} - 4\Phi_{i,j})/h^2. \quad (17)$$

The integrals $\int d^2\rho$ in Eqs. (12) and (13) are replaced by $h^2 \sum_{i,j}$. The operator \hat{L}_h is chosen to be equivalent to $\nabla_{\boldsymbol{\rho}}^2$ at low momenta $p \ll 1/h$. Although the lattice model gives a way to calculate observables in terms of g and h , the final results will be expressed in terms of the unique parameter B_2 . The relation among B_2 , g , and h is established by solving the lattice dimer problem. For vanishing center-of-mass momentum we have [24]

$$\frac{1}{g} = -\frac{1}{2\pi(1 + |B_2|h^2/4)} \mathbf{K} \left[\frac{1}{1 + |B_2|h^2/4} \right] \approx \frac{\ln(|B_2|h^2/32)}{4\pi} - \frac{|B_2|h^2}{32\pi} \ln(|B_2|h^2e/32), \quad (18)$$

where $\mathbf{K}(\kappa) = \int_0^{\pi/2} d\phi / \sqrt{1 - \kappa^2 \sin^2 \phi}$ is the complete elliptic integral. The first equality in Eq. (18) is exact and the last expression contains the usual logarithmically running term plus the leading effective-range correction.

The lattice and continuum models are equivalent at low momenta $p \ll 1/h$ and describe the same energies and wave functions of the low-lying Bogoliubov excitations. Therefore, the beyond-mean-field correction can be represented as an h -independent constant term plus a term logarithmic in h , determined by the high-momentum part of the integral in Eq. (16) cut off at $p \sim 1/h$. In fact, by rescaling the coordinate in Eq. (14) one can show that the beyond-mean-field correction is a product of $1/R^2$ and a function of h/R , which, as we have just argued, is logarithmic when $h/R \ll 1$. Accordingly, we write E_{BMF} as

$$E_{\text{BMF},h} = -\frac{N^2 g_c^2}{4\pi^2 C R^2} \ln(\xi R/h) = -\frac{C}{4R^2} \ln(\xi R/h), \quad (19)$$

where ξ is a dimensionless number and we use Eq. (5) when integrating Eq. (16) over $\boldsymbol{\rho}$.

For stationary Townes solitons described by Eq. (3) (with $g = g_c$) the kinetic and interaction energies equal, respectively, $N/2R^2$ and $-N/2R^2$, which we identify as the mean-field energy scale. We see that the beyond-mean-field correction (19) is of order $1/R^2$, i.e., smaller than the mean-field scale by a factor $1/N \ll 1$. Here we operate at this leading-order beyond-mean-field accuracy and neglect subleading terms. With this assumption we can still trust Eq. (19) when $g \neq g_c$ as long as $|g - g_c|/|g_c| \lesssim 1/N$. We also assume that the soliton size changes sufficiently slowly, such that quantum correlations and the energy of the Bogoliubov vacuum expressed by Eq. (15) have time to adiabatically adapt to this evolution. We write this constraint as

$$|\dot{R}(t)/R(t)| \ll 1/R^2(t), \quad (20)$$

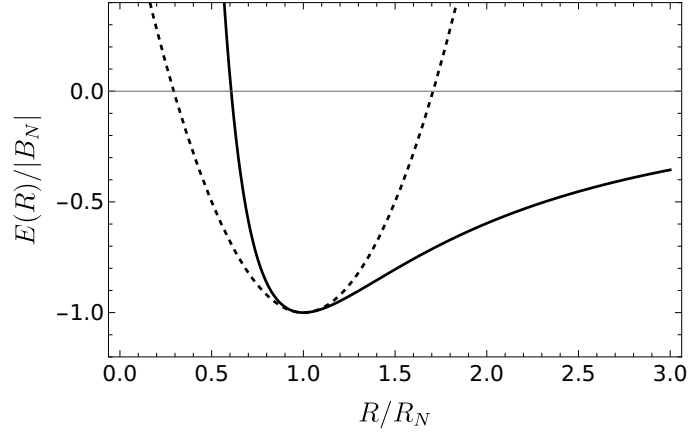


Figure 1: The potential $E(R)$ (solid) describing the breathing dynamics. The dashed curve shows the harmonic approximation valid near the equilibrium point.

where the rate of change of the condensate wave function on the left-hand side is compared to the time it takes for a typical Bogoliubov excitation to pass through the droplet [23]. Under these conditions we can predict the size and energy of the N -body soliton and describe its breathing dynamics.

3.1 Ground-state properties

The energy of the soliton of size R including the mean-field and leading beyond-mean-field terms equals

$$E(R) = \frac{(g - g_c)N^2}{2\pi C R^2} - \frac{C}{4R^2} \ln(\xi R/h) = -\frac{N}{2R^2} - \frac{C}{4R^2} \ln \xi \sqrt{|B_2|} R, \quad (21)$$

where we use $g - g_c = gg_c(1/g_c - 1/g) \approx g_c^2(1/g_c - 1/g)$ and Eq. (18) neglecting the effective-range term. Note that h and g drop out of the problem. Equation (21) has a minimum at

$$R_N = \frac{1}{\sqrt{|B_2|}} e^{-2N/C + 1/2 + \ln(4\sqrt{2}/\xi)} \quad (22)$$

with the energy

$$B_N = E(R_N) = -\frac{C}{8R_N^2} = B_2 e^{4N/C - 1 - 8\ln 2 + \ln(C\xi^2)}. \quad (23)$$

The main exponential dependence on N in Eqs. (22) and (23) has been predicted by Hammer and Son [13]. Here we derive the next-order correction and establish that the quantity $\ln(B_N/B_2) - 4N/C$ tends to $c_1 = -1 - 8\ln 2 + \ln(C\xi^2) = -1.91(1)$. To find this constant we numerically diagonalize the lattice version of Eq. (14), substitute the spectrum into Eq. (15), and fit the result with Eq. (19) for $h/R \ll 1$. More details on this calculation is provided in Appendix A. Note that ξ is specific to the chosen regularization method (square lattice), whereas c_1 is a universal number characterizing the zero-range model.

3.2 Breathing dynamics

We now discuss how the breathing dynamics is affected by the beyond-mean-field correction (21). To this end we use the action (11) with the mean-field energy replaced by $E(R)$

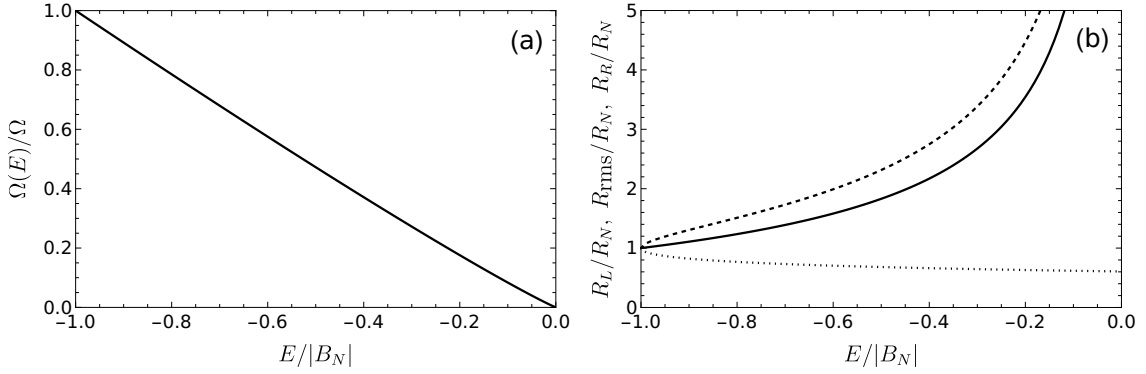


Figure 2: (a) The frequency $\Omega(E)$ of finite-amplitude breathing oscillations as a function of the total energy E of the system in units of $|B_N|$. The limit $E \rightarrow -|B_N|$ corresponds to vanishing amplitude, where $\Omega(E) = \Omega$. At the threshold $E = 0$ the soliton has just enough energy to expand to $R \rightarrow \infty$. (b) Other parameters of finite-amplitude oscillations: the left and right turning points R_L (dotted) and R_R (dashed) and the rms radius R_{rms} (solid), obtained by averaging $R^2(t)$ over one oscillation period.

given by Eq. (21). Omitting the constant term in the action and using Eqs. (22) and (23) we obtain

$$S = \int dt \left[\frac{NM_2}{C} \frac{\dot{R}^2(t)}{2} - E[R(t)] \right] = \int dt \left[\frac{NM_2}{C} \frac{\dot{R}^2(t)}{2} + 2|B_N| \frac{R_N^2}{R^2(t)} \ln \frac{R(t)e^{1/2}}{R_N} \right] \quad (24)$$

In Fig. 1 we show the potential $E(R)$. In contrast to the mean-field breathing dynamics discussed in Sec. 2, we now deal with a finite oscillating breathing motion. The dashed curve in Fig. 1 shows the harmonic approximation $E(R) \approx -|B_N| + 2|B_N|(R - R_N)^2/R_N^2$ valid in the vicinity of the equilibrium radius. Small-amplitude oscillations are characterized by the frequency

$$\Omega = \frac{4\sqrt{2}}{\sqrt{NM_2}} |B_N|, \quad (25)$$

where M_2 is defined in Eq. (6). On the other hand, as one can see from Fig. 1, the harmonic approximation breaks down already for relatively small amplitudes and the oscillation period depends on the excitation amplitude.

Figure 2 illustrates some properties of the breathing dynamics. In Fig. 2(a) we show the finite-amplitude oscillation frequency $\Omega(E)$ in units of Ω as a function of the conserved total energy of the system $E = NM_2\dot{R}^2/2C + E(R)$ in units of $|B_N|$. Small-amplitude oscillations correspond to $E \approx -|B_N|$. The amplitude increases and the frequency decreases with E . When E approaches zero the oscillation period diverges and the droplet spends lots of time at large R . In Fig. 2b we show the left turning radius R_L (dotted), the root mean square radius R_{rms} (solid), and the right turning radius R_R (dashed) as a function of E .

One can check that for any fixed $E < 0$ and for sufficiently large N the bound periodic trajectories $R(t)$ satisfy the adiabaticity condition (20). However, for fixed N this condition breaks down at small $|E|$ (see Sec. 4).

To give an idea of realistic time and length scales let us write the full period of small-amplitude oscillations in the dimensional form $\tau = 2\pi/\Omega = 7.1mR_N^2\sqrt{N}/\hbar$. Applying this formula to Cs (we have in mind the quasi-two-dimensional experiments of Chen and Hung [4,6]) we obtain $\tau \approx 100\text{ms}$ for $N = 16$ and $R_N = 1.3\mu\text{m}$. The corresponding peak density is approximately 4 atoms per μm^2 .

4 Discussion

Although the mechanism leading to these finite-frequency oscillations is quantum, the dynamics discussed so far in the limit $N \rightarrow \infty$ is classical. Let us try to go one step further and imagine what happens when we quantize the classical model (24). First of all, it is clear that in this case the breathing excitations form a discrete ladder. The number of states in this ladder increases with N since the ratio of the level spacing to the well depth $\sim \Omega(E)/|B_N|$ decreases as $1/\sqrt{N}$. Moreover, because of the thick tail of the potential $E(R) \propto -R^{-2} \ln(R/R_N)$ one may even think that there is an infinite number of bound states accumulated just under the threshold $E = 0$. This argument cannot be trusted in view of the fact that the adiabaticity condition (20) gets violated for $R \gtrsim R_N e^{\sqrt{N}}$. This estimate comes from the result $\dot{R}/R \propto R^{-2} N^{-1/2} \ln R/R_N$ obtained for $E = 0$ by equating the kinetic energy $\propto N \dot{R}^2$ and $-E(R)$. Note that for $N = 3$ and $N = 4$ there is only one excited state and an abrupt change from finite number of states to infinite number of states at a certain N seems unrealistic. We thus conjecture that there is a sequence of critical N at which the number of bound states increases by one. We point out that the states are not equidistant, and the quantum breathing dynamics may be quite different from the classical one governed by the periodic trajectory $R(t)$.

Quantization of the breathing mode leads to another interesting observation. Bazak and Petrov [17] have calculated B_N for $N \leq 26$ and tried to fit their data with the series expansion $\ln(B_N/B_2) - 4N/C = c_1 + c_2/N + c_3/N^2 + \dots$. This expansion is a natural generalization of the perturbative expansion in integer powers of g (in our case $|g| \sim 1/N$) discussed in the repulsive case [25]. We now see that this conjecture is likely to be wrong for the attractive case as the zero-point energy of the breathing mode $\Omega/2$ scales as $1/\sqrt{N}$ suggesting the presence of half-integer powers of $1/N$ in the series. Just adding $\Omega/2$ to B_N and using Eqs. (23) and (25) leads to

$$B_N \rightarrow B_N + \Omega/2 \approx B_2 e^{4N/C + c_1 - 2\sqrt{2}/\sqrt{M_2 N}}. \quad (26)$$

To check this scenario, in Fig. 3 we show the data of Ref. [17] in the form $\ln(B_N/B_2) - 4N/C - c_1$ (where we use $c_1 = -1.9067$) as a function of $1/\sqrt{N}$ together with the line $-2\sqrt{2}/\sqrt{NM_2}$ (dashed). We see that the presence of the $1/\sqrt{N}$ term is a reasonable hypothesis, also consistent with the fact that $c_1 = -1.91(1)$ found here is rather far from $c_1 \approx -2.06(4)$, obtained in Ref. [17] assuming only integer powers. For firmly proving or disproving this hypothesis one needs to reach higher values of N , which is possible with current numerical techniques [26].

In some sense the quantum zero-point motion of the collective coordinate R can be considered as a partial restoration of the mean-field Pitaevskii-Rosch scaling symmetry. Obviously, the other symmetries [translational and $U(1)$] are completely unbroken in the quantum case and the corresponding coordinates should remain completely delocalized. Quantizing the corresponding modes, as we have just done for the breathing mode, we would get vanishing zero-point energies. This is why our symmetry-breaking Bogoliubov method is sufficient for determining the energy at the leading-order beyond-mean-field level. This statement may still seem surprising since a general number-nonconserving theory should in principle allow for increasing N and, therefore, exponentially descending in energy according to Eq. (23). The reason why the Bogoliubov approach works is that it does not allow significant changes of the wave function (large fluctuations of R). To remove any shadow of doubt we have directly checked that the number-conserving approach of Castin and Dum [22] predicts the same soliton energy. It may be useful to provide a few details here.

To zeroth order, the number-conserving theory of Ref. [22] assumes that the system

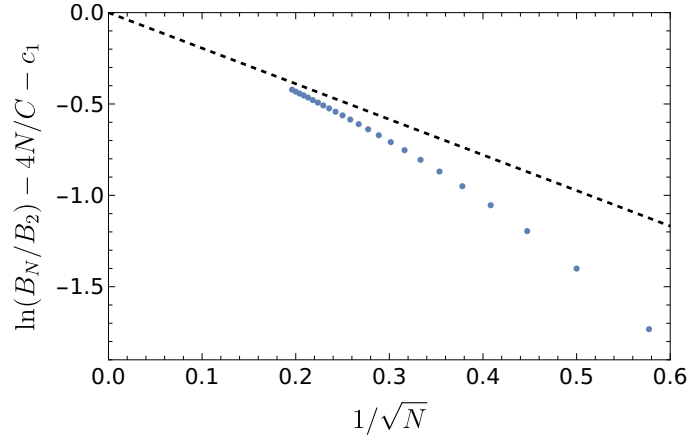


Figure 3: The quantity $\ln(B_N/B_2) - 4N/C - c_1$ as a function of $1/\sqrt{N}$. The data for B_N/B_2 are taken from Ref. [17] and the dashed line stands for $-2\sqrt{2}/\sqrt{NM_2}$, see Eq. (26).

is in the Fock state of N atoms occupying the single-particle orbital $|\Psi_R\rangle$ (normalized to 1). For $g = g_c$ the expectation value of the Hamiltonian (12) in this state equals $1/2R^2$, different from the vanishing mean-field energy in the symmetry-breaking approach. This difference results from the quantum-mechanical behavior of the operator $\hat{\Psi}_\rho^\dagger \hat{\Psi}_\rho^\dagger \hat{\Psi}_\rho \hat{\Psi}_\rho$ and from the fact that the expectation value of the interaction is proportional to the number of pairs $N(N-1)/2$ and not to $N^2/2$ as implied by the mean-field energy functional Eq. (7). The difference is at the beyond-mean-field level and one still needs to take into account other beyond-mean-field contributions. To this end Castin and Dum construct a quadratic Hamiltonian of type (13), but operating on excitations orthogonal to $|\Psi_R\rangle$. The result is Eq. (14), where the operators \hat{A} and \hat{B} are replaced by $\hat{Q}\hat{A}\hat{Q}$ and $\hat{Q}\hat{B}\hat{Q}$ and the operator $\hat{Q} = 1 - |\Psi_R\rangle\langle\Psi_R|$ projects onto single-particle states orthogonal to $\Psi_R(\rho)$. Castin and Dum explain that the nonzero part of the Bogoliubov spectrum is the same as in the symmetry-breaking approach. Therefore, the sum over eigenenergies in Eq. (15) is also the same. However, we check that the trace changes as $-\text{Tr}(\hat{Q}\hat{A}\hat{Q})/2 + \text{Tr}\hat{A}/2 = -1/2R^2$, which means that the two approaches indeed predict the same energy at the leading beyond-mean-field level.

5 Summary

In this paper we use the Bogoliubov theory to calculate the leading-order quantum correction to the energy of a two-dimensional soliton. Our calculations improve the accuracy of the previously known exponential scalings [13] by fixing the preexponential factors in Eqs. (22) and (23). We also study the classical breathing dynamics of the soliton and find that the frequency of small-amplitude oscillations scales as $\Omega \sim |B_N|/\sqrt{N}$ at large N . The very existence of this mode is a clear manifestation of the quantum anomaly discussed in Ref. [18], but now observable in free space. Quantum-mechanically, the breathing excitations form a ladder of states and we conjecture that their number increases one by one as we add particles to the soliton. We also conjecture that the leading beyond-Bogoliubov relative correction to the soliton energy scales as $1/\sqrt{N}$ and originates from zero-point fluctuations of the breathing mode. Proving these conjectures emerges as a sound project for future studies.

Acknowledgment We are grateful to G. Astrakharchik, E. Demler, N. Pavloff, and A. Tononi for valuable discussions.

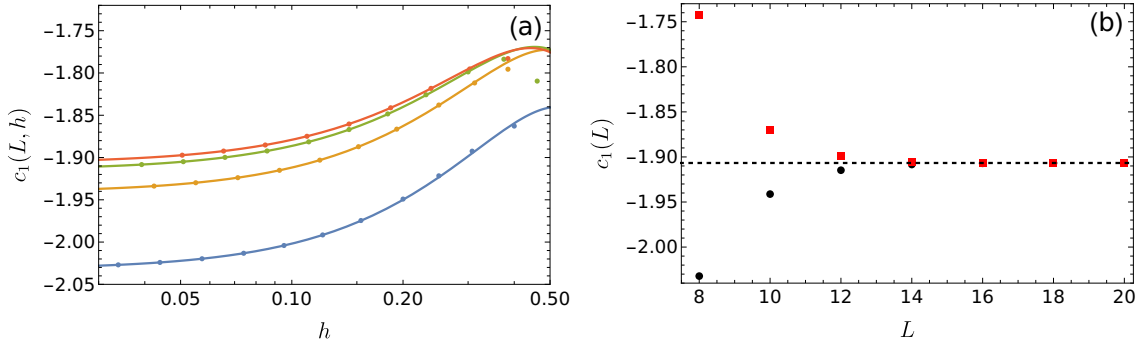


Figure 4: (a) The quantity $c_1(L, h)$ defined in Eq. (27) as a function of h for $L = 8$ (blue), 10 (yellow), 12 (green) and 20 (orange). The curves are fits by the functions $c_1(L) + \alpha(L)h^2 \ln[\beta(L)h]$. (b) The fitting parameter $c_1(L)$ as a function of L . The black circles and red squares correspond, respectively, to the Neumann and Dirichlet boundary conditions at the box boundaries. The horizontal dashed line shows $c_1 = -1.9067$.

A Determination of c_1

Our procedure for calculating ξ and determining the constant $c_1 = -1 - 8 \ln 2 + \ln(C\xi^2)$ in the large- N expansion $\ln(B_N/B_2) = 4N/C + c_1 + \dots$ is based on solving Eq. (14) on a square lattice with spacing h and external dimensions $L \times L$. More precisely, instead of Eq. (14) we diagonalize the matrix $(\hat{A} - \hat{B})(\hat{A} + \hat{B})$, eigenvalues of which are ϵ_ν^2 . The Laplacian is defined by Eq. (17) and, without loss of generality, we set $R = 1$. After diagonalization we use Eq. (15) to calculate the quantity

$$c_1(L, h) = -(8/C)E_{\text{BMF}}(L, h) - 1 - 8 \ln 2 + \ln C + 2 \ln h, \quad (27)$$

which, according to Eq. (19), should tend to c_1 , in the limit $h \rightarrow 0$, $L \rightarrow \infty$.

In our method we place the center of the soliton in the center of the box, which makes the system invariant with respect to reflections $x \rightarrow -x$ and $y \rightarrow -y$. These symmetries allow us to perform diagonalization only on the quarter of the box, i.e., for $x, y \in [0, L/2]$, although we then have to run the code for three different sets of boundary conditions on the eigenfunctions at the edges $x = 0$ and $y = 0$. In the first case we set the zero-derivative condition on both boundaries (Neumann-Neumann), in the second the zero-function boundary condition on both boundaries (Dirichlet-Dirichlet), and the third case corresponds to Neumann-Dirichlet configuration [the corresponding spectrum should be counted twice in Eq. (15)]. Moreover, to estimate finite size effects we repeat these calculations for two different sets of boundary conditions (Neumann and Dirichlet) at the external boundaries of the box.

In Fig. 4(a) we show $c_1(L, h)$ as a function of h for $L = 8, 10, 12$, and 20 obtained with the Neumann boundary condition at the external boundaries. Results look similarly for other values of L and for the Dirichlet boundary conditions, but we do not show them to avoid clutter. The solid curves are fits assuming $c_1(L, h) = c_1(L) + \alpha(L)h^2 \ln[\beta(L)h]$, where $c_1(L)$, $\alpha(L)$, and $\beta(L)$ are fitting parameters. The fits are based on the four leftmost data points (corresponding to the four smallest h), but as one can see, they work very well for significantly larger h . This form of fitting function is a typical effective-range expansion in a weakly-interacting regime in two dimensions. It shows up in the local-density analysis Eq. (16) when we replace p^2 by its lattice analog $[4 - 2 \cos(p_x h) - 2 \cos(p_y h)]/h^2$. The integral over $p_x, p_y \in [-\pi/h, \pi/h]$ is then similar to the one leading to Eq. (18), where the

effective-range term $\sim h^2 \ln h$ is shown explicitly. We have also seen this behavior in the numerical analysis of two-dimensional droplets in Ref. [27].

In Fig. 4(b) we plot the fitting parameter $c_1(L)$ as a function of L for the Neumann (black circles) and for the Dirichlet (red squares) boundary condition at the box edges. Both datasets exponentially converge to $c_1 = -1.9067$ (dashed horizontal line) with the exponent $\propto e^{-3L/4}$ (fits are not shown). We estimate the uncertainty of this final result as the difference between the extrapolated value $c_1(20.)$ and the value $c_1(20., 0.05)$, calculated for the largest L and smallest h . We thus claim $c_1 = 1.91(1)$.

References

- [1] R. Y. Chiao, E. Garmire, and C. H. Townes, Self-Trapping of Optical Beams, *Phys. Rev. Lett.* **13**, 479 (1964), DOI: <https://doi.org/10.1103/PhysRevLett.13.479>.
- [2] L. P. Pitaevskii and A. Rosch, Breathing modes and hidden symmetry of trapped atoms in two dimensions, *Phys. Rev. A* **55**, R853 (1997), DOI: <https://doi.org/10.1103/PhysRevA.55.R853>.
- [3] B. Bakkali-Hassani and J. Dalibard, Townes soliton and beyond: Non-miscible Bose mixtures in 2D, *Proceedings of the International School of Physics "Enrico Fermi", Course 211 - Quantum Mixtures with Ultra-cold Atoms, July 2022*, directors: Rudolf Grimm, Massimo Inguscio, Sandro Stringari.
- [4] C.-A. Chen and C.-L. Hung, Observation of Universal Quench Dynamics and Townes Soliton Formation from Modulational Instability in Two-Dimensional Bose Gases, *Phys. Rev. Lett.* **125**, 250401 (2020), DOI: [10.1103/PhysRevLett.125.250401](https://doi.org/10.1103/PhysRevLett.125.250401).
- [5] B. Bakkali-Hassani, C. Maury, Y.-Q. Zou, É. Le Cerf, R. Saint-Jalm, P. C. M. Castilho, S. Nascimbene, J. Dalibard, and J. Beugnon, Realization of a Townes Soliton in a Two-Component Planar Bose Gas, *Phys. Rev. Lett.* **127**, 023603 (2021), DOI: <https://doi.org/10.1103/PhysRevLett.127.023603>.
- [6] C.-A. Chen and C.-L. Hung, Observation of Scale Invariance in Two-Dimensional Matter-Wave Townes Solitons, *Phys. Rev. Lett.* **127**, 023604 (2021), DOI: <https://doi.org/10.1103/PhysRevLett.127.023604>.
- [7] S. N. Vlasov, V. A. Petrishchev, and V. I. Talanov, Averaged description of wave beams in linear and nonlinear media, *Izv. Vyssh. Uchebn. Zaved. Radiofiz.* **14**, 1353 (1971), DOI: <https://doi.org/10.1007/BF01029467>.
- [8] L. P. Pitaevskii, Dynamics of collapse of a confined Bose gas, *Phys. Lett. A* **221**, 14 (1996), DOI: [https://doi.org/10.1016/0375-9601\(96\)00538-5](https://doi.org/10.1016/0375-9601(96)00538-5).
- [9] L. W. Bruch and J. A. Tjon, Binding of three identical bosons in two dimensions, *Phys. Rev. A* **19**, 425 (1979), DOI: <https://doi.org/10.1103/PhysRevA.19.425>.
- [10] S. K. Adhikari, A. Delfino, T. Frederico, I. D. Goldman, and L. Tomio, Efimov and Thomas effects and the model dependence of three-particle observables in two and three dimensions, *Phys. Rev. A* **37**, 3666 (1988), DOI: <https://doi.org/10.1103/PhysRevA.37.3666>.
- [11] E. Nielsen, D. V. Fedorov, and A. S. Jensen, Three-body halos in two dimensions, *Phys. Rev. A* **56**, 3287 (1997), DOI: <https://doi.org/10.1103/PhysRevA.56.3287>.

- [12] E. Nielsen, D. V. Fedorov, and A. S. Jensen, Structure and Occurrence of Three-Body Halos in Two Dimensions, *Few-Body Systems* **27**, 15 (1999), DOI: <https://doi.org/10.1007/s006010050121>.
- [13] H.-W. Hammer and D. T. Son, Universal properties of two-dimensional boson droplets, *Phys. Rev. Lett.* **93**, 250408 (2004), DOI: <https://doi.org/10.1103/PhysRevLett.93.250408>.
- [14] L. Platter, H.-W. Hammer, and U.-G. Meißner, Universal Properties of the Four-Boson System in Two Dimensions, *Few-Body Syst.* **35**, 169 (2004), DOI: <https://doi.org/10.1007/s00601-004-0065-z>.
- [15] I. V. Brodsky, M. Yu. Kagan, A. V. Klapptsov, R. Combescot, and X. Leyronas, Exact diagrammatic approach for dimer-dimer scattering and bound states of three and four resonantly interacting particles, *Phys. Rev. A* **73**, 032724 (2006), DOI: <https://doi.org/10.1103/PhysRevA.73.032724>.
- [16] O. I. Kartavtsev and A. V. Malykh, Universal low-energy properties of three two-dimensional bosons, *Phys. Rev. A* **74**, 042506 (2006), DOI: <https://doi.org/10.1103/PhysRevA.74.042506>.
- [17] B. Bazak and D. S. Petrov, Energy of N two-dimensional bosons with zero-range interactions, *New J. Phys.* **20**, 023045 (2018), DOI: <https://doi.org/10.1088/1367-2630/aaa64f>.
- [18] M. Olshanii, H. Perrin, and V. Lorent, Example of a Quantum Anomaly in the Physics of Ultracold Gases, *Phys. Rev. Lett.* **105**, 095302 (2010), DOI: <https://doi.org/10.1103/PhysRevLett.105.095302>.
- [19] That the quantity $\ln(B_N/B_2) - 2N/C$ tends to a constant at large N is a reasonable conjecture, but, in principle, it could be any $o(N)$ function, like \sqrt{N} or $\ln N$.
- [20] J.-P. Blaizot and G. Ripka, *Quantum Theory of Finite Systems*, MIT Press, Cambridge, MA, ISBN 0262022141 (1986).
- [21] M. Lewenstein and L. You, Quantum Phase Diffusion of a Bose-Einstein Condensate, *Phys. Rev. Lett.* **77**, 3489 (1996), DOI: <https://doi.org/10.1103/PhysRevLett.77.3489>.
- [22] Y. Castin and R. Dum, Low-temperature Bose-Einstein condensates in time-dependent traps: Beyond the $U(1)$ symmetry-breaking approach, *Phys. Rev. A* **57**, 3008 (1998), DOI: <https://doi.org/10.1103/PhysRevA.57.3008>.
- [23] The Bogoliubov spectrum of the soliton is continuous and its level spacing goes to zero as we increase the box size L . However, in Appendix A we show that the beyond-mean-field correction (15) becomes exponentially insensitive to L as long as $L \gtrsim R$, i.e., when the soliton no longer touches the walls. The quantity $1/R^2$ on the right-hand side of the inequality (20) is of order the level spacing in an imaginary box of size $\sim R$.
- [24] P. E. Kornilovitch, Two-particle bound states on a lattice, *Ann. Phys.* **460**, 169574 (2024), DOI: [10.1016/j.aop.2023.169574](https://doi.org/10.1016/j.aop.2023.169574).
- [25] C. Mora and Y. Castin, Ground State Energy of the Two-Dimensional Weakly Interacting Bose Gas: First Correction Beyond Bogoliubov Theory, *Phys. Rev. Lett.* **102**, 180404 (2009), DOI: [10.1103/PhysRevLett.102.180404](https://doi.org/10.1103/PhysRevLett.102.180404).

- [26] A. Tononi, G. E. Astrakharchik, and D. S. Petrov, Gas-to-soliton transition of attractive bosons on a spherical surface, AVS Quantum Sci. **6**, 023201 (2024), DOI: <https://doi.org/10.1116/5.0190767>.
- [27] D. S. Petrov and G. E. Astrakharchik, Ultradilute Low-Dimensional Liquids, Phys. Rev. Lett. **117**, 100401 (2016), DOI:10.1103/PhysRevLett.117.100401.